Theoret. Appl. Mech., Vol.35, No.1-3, pp. 287–304, Belgrade 2008

Hysteretic behavior modeling of elastoplastic materials

Dragoslav Šumarac * **Bojan Medjo** †
Nataša Trišović ‡

Abstract

In the present paper the Preisach model of hysteresis is applied to model cyclic behavior of elasto-plastic material. Rate of loading and viscous effects will not be considered. The problem of axial loading of rectangular cross section and cyclic bending of rectangular tube (box) will be studied in details. Hysteretic stress-strain loop for prescribed history of stress change is plotted for material modeled by series connection of three unite element. Also moment-curvature hysteretic loop is obtained for a prescribed curvature change of rectangular tube (box). One chapter of the paper is devoted to results obtained by FEM using Finite Element Code ABAQUS. All obtained results clearly show advantages of the Preisach model for describing cyclic behavior of elasto-plastic material.
Keywords: cyclic plasticity, Preisach model, cyclic bending

1 Introduction

Mathematical modeling of engineering materials is important issue in design of structures. Model itself should satisfy two conditions: first to explain in the best way mechanical behavior of material and second to be as simple as possible for easy every day application in engineering. In the present paper the model of elastic-plastic behavior for quasi static cyclic loading will be explained. Special

*Faculty of Civil Engineering, University of Belgrade, Bulevar Kralja Aleksandra 73, 11000 Belgrade, Serbia, e-mail: sumi@grf.bg.ac.yu, sumi@grf.bg.ac.yu

†Faculty of Technology and Metallurgy, University of Belgrade, Karnegijeva 4, 11000 Belgrade, Serbia, e-mail: bojanmedjo@gmail.com, bojanmedjo@gmail.com

‡Faculty of Mechanical Engineering, University of Belgrade, Kraljice Marije 16, 11000 Belgrade, Serbia, e-mail: ntrisovic@mas.bg.ac.yu, ntrisovic@mas.bg.ac.yu

attention will be made to hysteretic behavior and mathematical models applied for their description. Constitutive relations will not include viscous effects and rate of loading application. In this paper moment-curvature loops will be constructed for cyclic axial loading and cyclic bending, respectively. From these examples it is obvious that suggested (Preisach) model is simple enough and very appropriate to describe hysteretic behavior of elasto-plastic material.

2 The Preisach model of hysteresis

The Preisach model of hysteresis, dealing with the problem of magnetism, is described thoroughly in the monograph of Mayergoyz [7]. The phenomenon of hysteresis occurs in various branches of physics: mechanics, magnetism, optics, adsorption etc. Application of the Preisach model to cyclic behavior of elasto-plastic material is shown in [5] and extended to cyclic bending by [3]. In this paper short outline of Preisach model of hysteresis will be presented. According to [7], the Preisach model implies the mapping of an input of strain $\varepsilon(t)$ on the output of stress $\sigma(t)$ in the integral form:

$$\sigma(t) = \iint P(\alpha, \beta)\, G_{\alpha,\beta}\varepsilon(t)\, d\alpha d\beta \tag{1}$$

where $G_{\alpha,\beta}$ is an elementary hysteresis operator given in Fig.1.

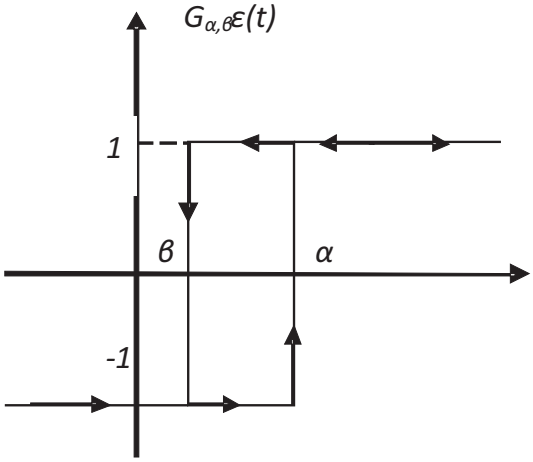

Figure 1: Elementary hysteresis operator

Parameters α and β are up and down switching values of the input, while $P(\alpha, \beta)$ is the Preisach function, i.e. a weight (Green's) function of the hysteresis nonlinearity to be represented by the Preisach model. The domain of

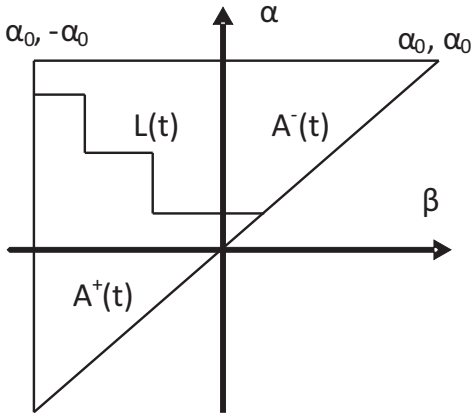

Figure 2: Limiting triangle with the interface staircase line $L(t)$

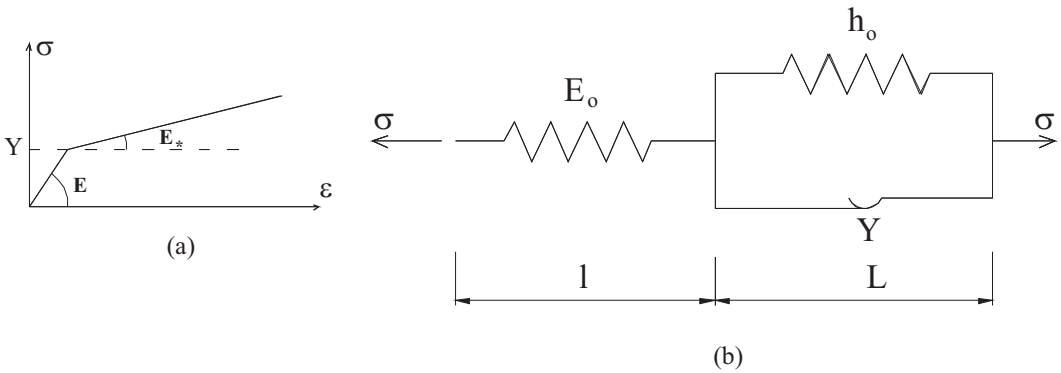

Figure 3: (a) Elastic-linearly hardening stress-strain behaviour with elastic modulus E, initial yield stress Y and hardening modulus E_h; (b) Three-element unit reproducing the stress-strain behaviour in (a)

integration of integral (1) is right triangle in the α, β plane, with $\alpha = \beta$ being the hypotenuse and (α_0,$\beta_0 = -\alpha_0$) being the triangular vertex (Fig.2). History of loading corresponds to staircase line $L(t)$ which divides triangle into two parts [5]. Maxima or minima of loading history are represented by the vertices with coordinates (α, β) on staircase line $L(t)$ in such a way if the input at a previous instant of time is increased, the final link of $L(t)$ is horizontal, and vise versa if it is decreased it is vertical. Therefore, the triangle is divided into two parts with the positive and negative values of $G_{\alpha,\beta}$ by the interface

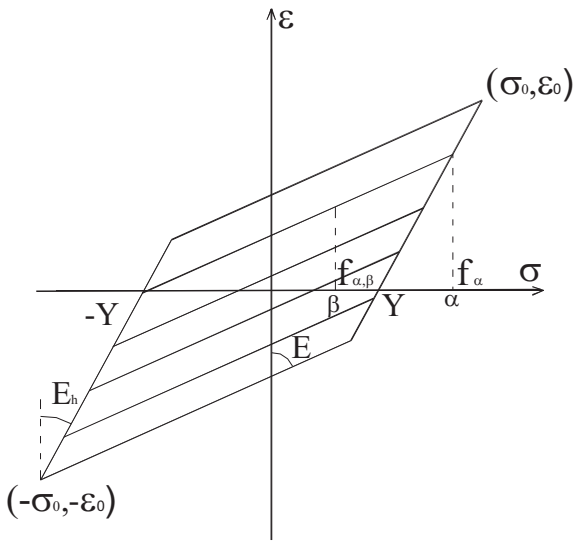

Figure 4: Major hysteresis loop and several transition lines, corresponding to the material model in Fig. 3.

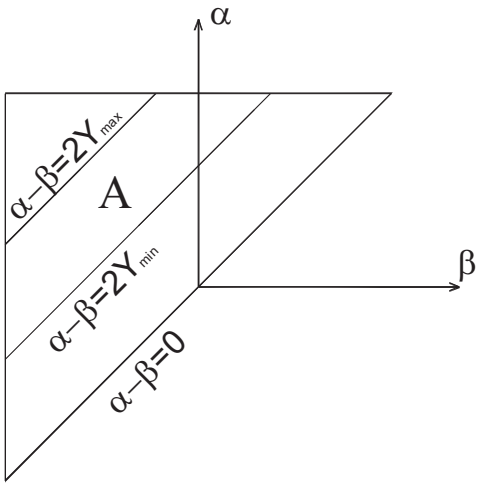

Figure 5: The Preisach function corresponding to series connection of infinitely many three element units

staircase line $L(t)$. From formula (1) it is than obtained:

$$\sigma(t) = \iint\limits_{A^+(t)} P(\alpha,\beta)\, G_{\alpha,\beta\varepsilon}(t)\, d\alpha d\beta - \iint\limits_{A^-(t)} P(\alpha,\beta)\, G_{\alpha,\beta\varepsilon}(t)\, d\alpha d\beta \qquad (2)$$

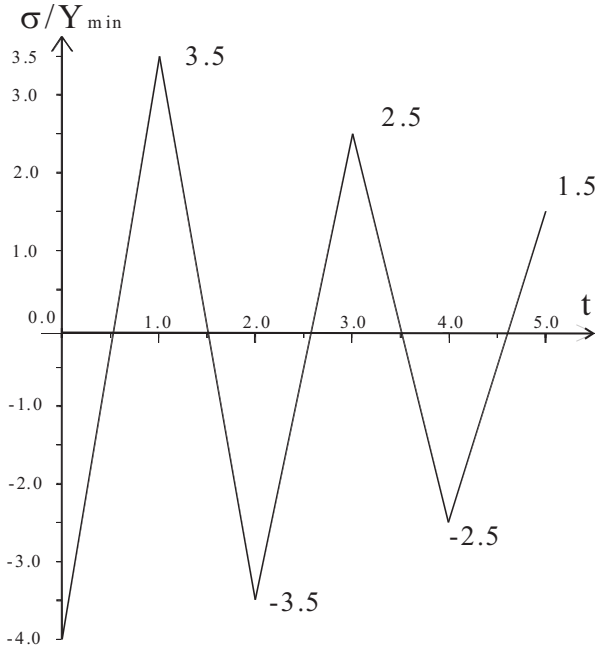

Figure 6: History of stress input

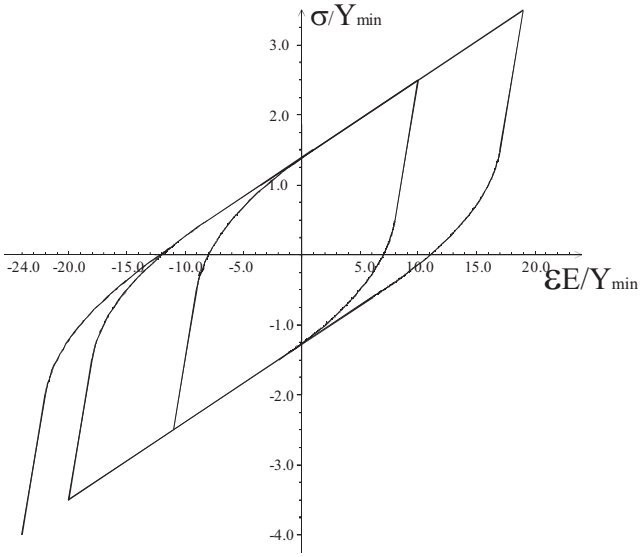

Figure 7: Stress-strain loop

Denoting the output value at $\varepsilon = \beta$ by $f_{\alpha,\beta}$ from the limiting triangle, it

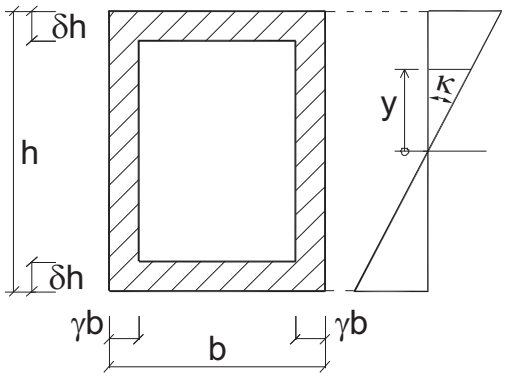

Figure 8: Rectangular tube (box) cross section

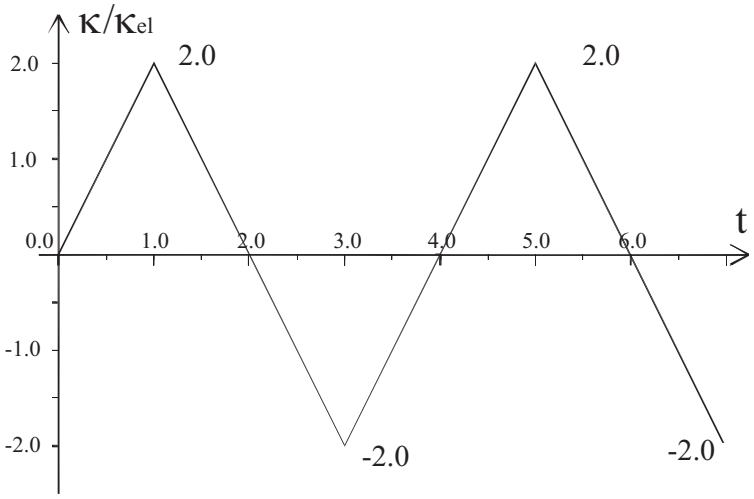

Figure 9: History of curvature change

follows that

$$f_{\alpha,\beta} - f_{\alpha} = -2 \int_{\beta}^{\alpha} \left(\int_{\beta}^{'\alpha} P\left(\alpha', \beta'\right) d\alpha' \right) d\beta' \tag{3}$$

By differentiating expression (3) twice, with respect to α and β, the Preisach weight function is derived in the form

$$P\left(\alpha, \beta\right) = \frac{1}{2} \frac{\partial^2 f_{\alpha,\beta}}{\partial \alpha \partial \beta} \tag{4}$$

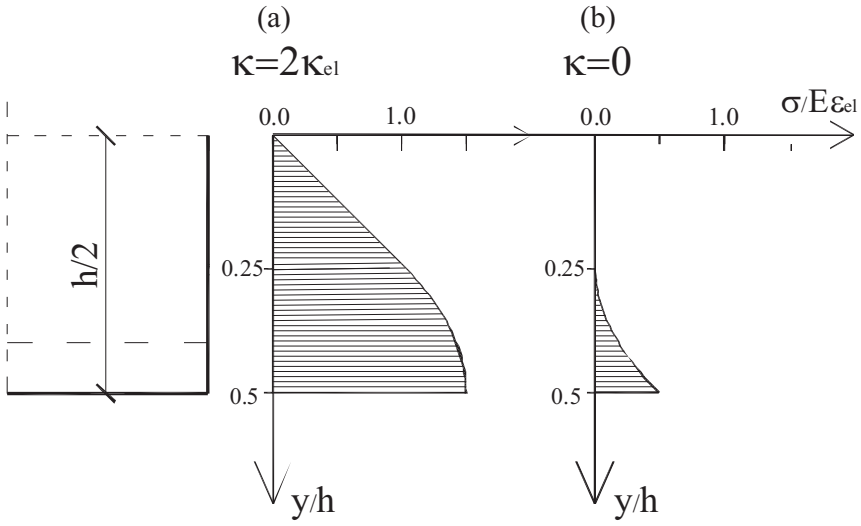

Figure 10: Residual stresses (a) for $\kappa = 2\kappa_{el}$, (b) for $\kappa = 0$

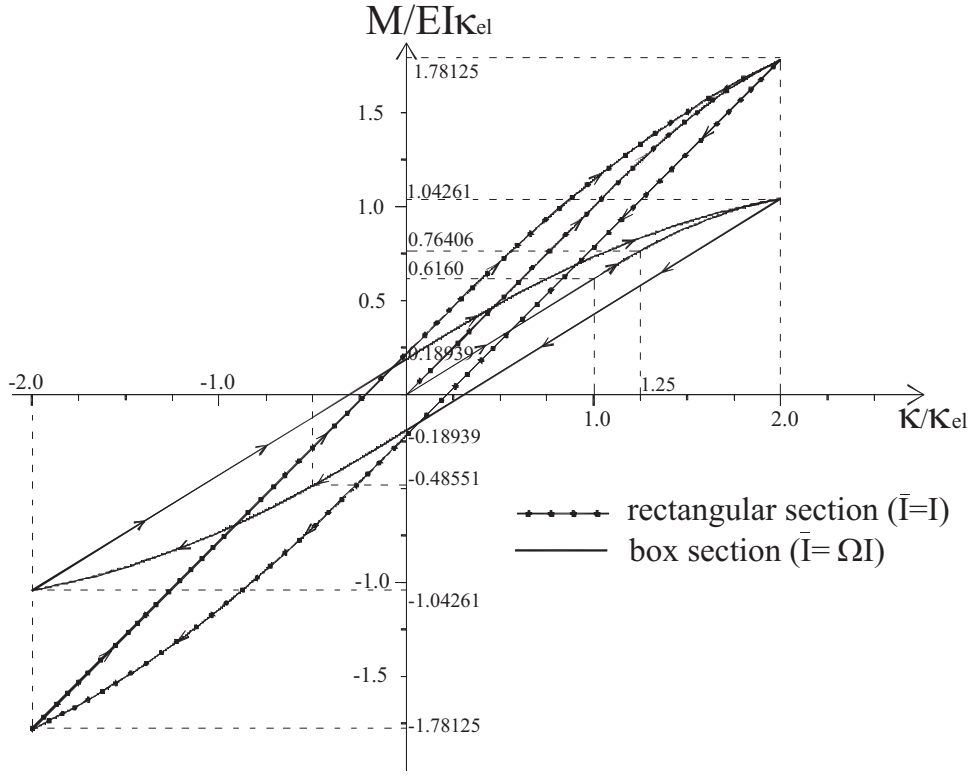

Figure 11: Moment curvature loop

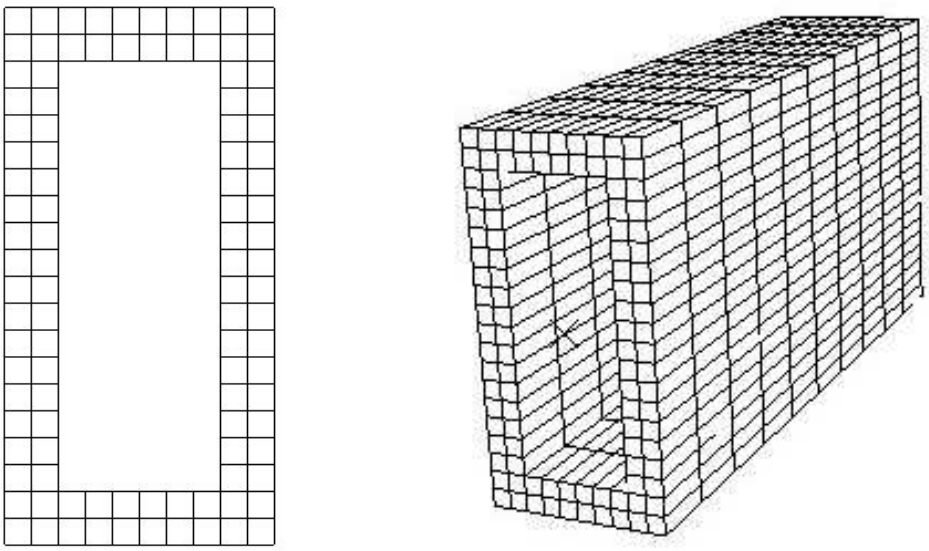

Figure 12: FE mesh

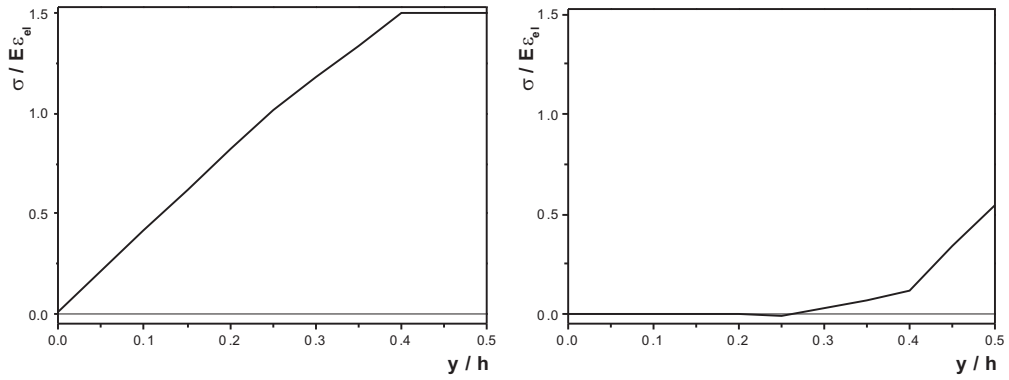

Figure 13: Residual stresses (a) for $\kappa = 2\kappa_{el}$, (b) for $\kappa = 0$ - numerically obtained

The Preisach model explained above possesses two properties: wiping out and congruency properties. Those properties and much more about Preisach model is explained in [5] and [6].

3 The Preisach model for cyclic behavior of ductile materials

One dimensional hysteretic behavior of elasto-plastic material can be successfully described by the Preisach model. Ductile material is represented in various ways by a series or parallel connections of elastic (spring) and plastic (slip) elements [6]. These results have advantage in comparison with classically obtained [4] and [1] because of simplicity and strict mathematical rigorous procedure. Parallel Connection of elastic and slip elements, Series connection of elastic and slip elements are discussed elsewhere [3], [6]. Here we will consider a three element unit.

3.1 A three-element unit

Elastic-linearly hardening material behavior, characterized by the stress-strain curve shown in Fig.3a. (E and E_h are elastic and hardening moduli), can be modeled by a three-element unit shown in Fig.3b. Elastic element of length l and modules E_0 is connected in a series with a parallel connection of elastic and slip element, of length L modulus h_0 and yield strength Y. It then follows that $E = E_0(l + L)/l$ and $E_h = Eh\,(E + h)$, where $h = h_0(l + L)/L$. The Preisach function can be determined from the hysteresis nonlinearity shown in Fig.4, which relates the stress input to strain output. The Preisach function in this case has support along the lines $\alpha - \beta = 0$ and $\alpha - \beta = 2Y$, i.e. it is given by

$$P\,(\alpha, \beta) = \frac{1}{2E}\left[\delta\,(\alpha - \beta) + \frac{E - E_h}{E_h}\delta\,(\alpha - \beta - 2Y)\right]. \tag{5}$$

The expression for strain as a function of applied stress is, consequently,

$$\varepsilon\,(t) = \frac{1}{2E}\left[\int_{-\sigma_0}^{\sigma_0} G_{\alpha,\alpha}\sigma\,(t)\,d\alpha + \frac{E - E_h}{E_h}\int_{2Y-\sigma_0}^{\sigma_0} G_{\alpha,\alpha-2Y}\sigma\,(t)\,d\alpha\right], \tag{6}$$

The first and second term on the right-hand side of (6) are elastic and plastic strain, respectively. For a system consisting of infinitely many of three-element units, connected in a series and with uniform yield strength distribution within the range $Y_{\min} \leqslant Y \leqslant Y_{\max}$, the total strain is

$$\varepsilon\,(t) = \frac{1}{2E}\left[\int_{-\sigma_0}^{\sigma_0} G_{\alpha,\alpha}\sigma\,(t)\,d\alpha + \frac{E - E_h}{2E_h}\frac{1}{Y_{\max} - Y_{\min}}\int\int_A G_{\alpha,\beta}\sigma(t)d\alpha d\beta\right]. \tag{7}$$

In (7) the integration domain A is the area of the band contained between the lines $\alpha - \beta = 2Y_{\min}$ and $\alpha - \beta = 2Y_{\max}$ in the limiting triangle, shown in Fig.5. The first term on the right-hand side of (7) is the elastic strain, which can be written as $\sigma(t)/E$.

In the case when the strain is the input and stress output, the Preisach function becomes

$$P(\alpha, \beta) = \frac{E}{2}\delta(\alpha - \beta) - \frac{1}{2}(E - E_h)\,\delta\left(\alpha - \beta - 2\frac{Y}{E}\right). \tag{8}$$

The stress expression is form (1)

$$\sigma(t) = \frac{E}{2}\int\limits_{-\varepsilon_0}^{\varepsilon_0} G_{\alpha,\alpha}\varepsilon(t)d\alpha - \frac{1}{2}(E - E_h)\int\limits_{2\frac{Y}{E}-\varepsilon_0}^{\varepsilon_0} G_{\alpha,\alpha-2\frac{Y}{E}}\varepsilon(t)\,d\alpha. \tag{9}$$

3.2 Illustrative example

To illustrate the application of the Preisach model the stress-strain hysteretic curve is determined for material model of series connection of three unite element introduced in the previous subsection. In the calculation it is used $E_h = E/9$ and $Y_{max} = 2Y_{min}$. The loading history of stress change is shown in Fig.6. From the procedure explained above the strain in the first portion $-4Y_{min} < \sigma < -2Y_{min}$ is linear:

$$\frac{\varepsilon E}{Y_{\min}} = -20 + \frac{\sigma}{Y_{\min}} \tag{10}$$

For further increase of stresses in the region $-2Y_{min} < \sigma < 0$, staircase line L falls into the band are A shown in Fig.5 and consequently response is nonlinear:

$$\frac{\varepsilon E}{Y_{\min}} = -22 + \left(\frac{\sigma}{Y_{\min}} + 2\right)\left(5 + 2\frac{\sigma}{Y_{\min}}\right) \tag{11}$$

At the stress level $\sigma = 0$ the strongest element Y_{max} starts to yield. Saturation occurs and the system responds elastically with the Young's modulus $E_h = E/9$, i.e. in the region $0 < \sigma < 3.5Y_{min}$:

$$\frac{\varepsilon E}{Y_{\min}} = 9\frac{\sigma}{Y_{\min}} - 12.5 \tag{12}$$

In the region $1.5Y_{min} < \sigma < 3.5Y_{min}$ response is linear with the Young's modulus E:

$$\frac{\varepsilon E}{Y_{\min}} = 15.5 + \frac{\sigma}{Y_{\min}} \tag{13}$$

Further decrease of stresses, $-0.5Y_{min} < \sigma < 1.5Y_{min}$, leads to nonlinear response with the quadratic parabola:

$$\frac{\varepsilon E}{Y_{\min}} = 17 - \left(1.5 - \frac{\sigma}{Y_{\min}}\right)\left(4 - 2\frac{\sigma}{Y_{\min}}\right) \tag{14}$$

In the region, $-3.5Y_{min} < \sigma < -0.5Y_{min}$, saturation again occurs and the system responds as elastic with the Young's modulus of E_h:

$$\frac{\varepsilon E}{Y_{\min}} = 11.5 + 9\frac{\sigma}{Y_{\min}} \tag{15}$$

The further procedure is obvious, and the stress-strain loop is presented in Fig 7.

4 Cyclic bending of rectangular tube (box) beam

Uniaxial cyclic loading of bars, can be extended to cyclic bending of beams. In this paragraph symmetric pure bending of rectangular tube (box) cross section is considering (Fig.8). Taking into account Bernoulli's hypothesis one obtains strain as a function of y and intensity of curvature $\kappa(t)$ in the form:

$$\varepsilon(t) = \kappa(t)\, y \tag{16}$$

Substituting (16) into (1) yields to:

$$\sigma(y,t) = \iint\limits_{\alpha \geqslant \beta} P(\alpha,\beta)\, G_{\alpha,\beta}\left[\kappa(t)\, y\right] d\alpha d\beta \tag{17}$$

In expressions (16) and (17), $\kappa(t)$ is prescribed curvature change. The integration given by formula (17) is performed over the triangle that is dependent on the distance from the neutral fiber. Instead of having only one triangle, which represents the whole cross section in the case of axially loaded members, now every level y is represented by one limiting triangle. In this way the prism with a triangular base, which hereafter will be referred to as a Preisach prism, is obtained. Knowing stresses for arbitrary fiber given by y and defined by (17) the bending moment as a function of the curvature is obtained:

$$M(t) = \int\limits_a^b y\sigma(y,t)\, b(y)\, dy \tag{18}$$

Introducing expression (17) into (18) one obtains:

$$M(t) = \int_a^b yb(y)\frac{E}{2}\times$$

$$\left[\int_{-\varepsilon_L}^{\varepsilon_L} G_{\alpha,\alpha} y\kappa(t)\,d\alpha - \frac{E}{2(Y_{\max}-Y_{\min})}\iint_A G_{\alpha,\beta} y\kappa(t)\,d\alpha d\beta\right] dy \qquad (19)$$

In the above formulas a and b stand for distances of the lower and upper edges from the neutral fiber. Also material model is represented by parallel connection of infinitely many of elastic and slip elements connected in a series [3].

For a double symmetric cross section, such as the rectangular tub shown in Fig.8 for the prescribed history of curvature change shown in Fig.9, the neutral fiber is fixed at the center of the cross section. It is assumed that wall thickness of webs is γb and δh of vertical and horizontal one, respectively. Hence the moment of inertia is:

$$\bar{I} = I\Omega \qquad (20)$$

where

$$\Omega = 1 - (1-2\gamma)(1-2\delta)^3 \qquad (21)$$

and I stands for the moment of inertia of rectangular cross section:

$$\bar{I} = \frac{1}{12}bh^3 \qquad (22)$$

In the interval $0 < t < 0.5$, curvature is in the elastic range $0 < \kappa < \kappa_{el}$, where $\kappa_{el} = 2\varepsilon_{el}/h$ and the whole cross section is in the elastic range. From the expression (17) it is obtained: $\sigma(y,t) = E\kappa(t)y$. Integrating this result, using (4) yields to $M(t) = E\bar{I}\kappa(t)$. This linear diagram is shown in Figure 11. If the curvature is further increased, nonlinearity will appear. First nonlinearity will appear in the flange. So we have two regions:

$$\frac{\kappa_{el}}{\kappa} \geqslant 1-2\delta \qquad (23)$$

plasticity takes place in the flange, and for

$$\frac{\kappa_{el}}{\kappa} \leqslant 1-2\delta \qquad (24)$$

plasticity takes place in the vertical web.

In the region $0.5 < t < 1$, or $\kappa_{el} < \kappa < 2\kappa_{el}$, from (17) the stress at an arbitrary fiber is:

$$\sigma(y,t) = E\varepsilon_{el}\left[\frac{2\kappa(t)}{\kappa_{el}}\frac{y}{h} - H\left(y - \frac{\varepsilon_{el}}{\kappa}\right)2\left(\frac{k(t)}{\kappa_{el}}\frac{y}{h} - \frac{1}{2}\right)^2\right] \tag{25}$$

where H stands for the Heviside function. The diagram of the stress given by (25) is shown in Fig. 10a for $\kappa = 2\kappa_{el}$. Substituting (25) into (4) and integrating, the moment curvature relation is:

$$M(t) = E\bar{I}\kappa(t) - 3EI\kappa_{el}\left[\frac{1}{8}\frac{\kappa(t)^2}{k_{el}^2}\left(1 - \frac{\kappa_{el}^4}{\kappa(t)^4}\right)\right.$$
$$\left. -\frac{1}{3}\frac{\kappa(t)}{\kappa_{el}}\left(1 - \frac{\kappa_{el}^3}{k(t)^3}\right) + \frac{1}{4}\left(1 - \frac{\kappa_{el}^2}{k(t)^2}\right)\right] \tag{26}$$

Formula (26) is obtained for the case $\kappa_{el}\kappa > 1 - 2\delta$, i.e. plasticity takes place in the flange. This expression is the same as for I cross section, which is published in [3].

Increasing further curvature, in the region $\kappa_{el}\kappa < 1 - 2\delta$ elastic plastic boundary falls in the web. Then moment curvature relation is obtained from:

$$M = E\bar{I}\kappa - 6b\gamma E\varepsilon_{el}\int\limits_{\frac{\kappa_{el}}{\kappa}\frac{h}{2}}^{\frac{h}{2}(1-2\delta)}\left(\frac{\kappa(t)}{\kappa_{el}}\frac{y}{h} - \frac{1}{2}\right)^2 y dy -$$

$$4bE\varepsilon_{el}\int\limits_{\frac{h}{2}(1-2\delta)}^{\frac{h}{2}}\left(\frac{\kappa(t)}{\kappa_{el}}\frac{y}{h} - \frac{1}{2}\right)^2 y dy \tag{27}$$

After integration, final moment curvature relation reads:

$$M[\kappa(t)] = E\bar{I}\kappa(t) - 3EI\kappa_{el}\left\{\frac{1}{8}\frac{\kappa(t)^2}{\kappa_{el}^2}\left[1 - (1-2\gamma)(1-2\delta)^4 - 2\gamma\frac{\kappa_{el}^4}{\kappa(t)^4}\right]\right.$$
$$-\frac{1}{3}\frac{\kappa(t)}{\kappa_{el}}\left[1 - (1-2\gamma)(1-2\delta)^3 - 2\gamma\frac{\kappa_{el}^3}{\kappa(t)^3}\right]$$
$$\left. +\frac{1}{4}\left[1 - (1-2\gamma)(1-2\delta)^2 - 2\gamma\frac{\kappa_{el}^2}{\kappa(t)^2}\right]\right\} \tag{28}$$

Comparing this result with the result obtained in [3] for I cross section, they are the same except that 2γ in this paper should be replaced by γ and the result for I cross section is recovered.

From (28) it is easy to see that, in the case of rectangular cross section ($\delta = \gamma = 1/2$) for $\kappa = \kappa_{el}$, $M = EI\kappa_{el}$, while for $\kappa = 2\kappa_{el}$, $M = 1.78125EI\kappa_{el}$ which is the same as in [3].

For the history of loading in the interval $1 < t < 1.5$ or $0 < \kappa < 2\kappa_{el}$, the unloading starts. The Preisach prism doesn't change, except along the hypotenuse, and consequently the response is elastic. The stress is given by:

$$\sigma(y,t) = E\varepsilon_e \left[2\frac{\kappa(t)}{\kappa_{el}}\frac{y}{h} - H\left(y - \frac{h}{4}\right) 2\left(2\frac{y}{h} - \frac{1}{2}\right)^2 \right] \tag{29}$$

The most important thing that we can calculate from the expression (29) is the residual stress which is obtained for $\kappa = 0$:

$$\sigma(y, t = 1.5) = -E\varepsilon_{el} H\left(y - \frac{h}{4}\right) 2\left(2\frac{y}{h} - \frac{1}{2}\right)^2 \tag{30}$$

This diagram is plotted in Fig.10b. The moment-curvature relation in this region is linear:

$$M[\kappa(t)] = E\bar{I}\kappa - 3EI\kappa_{el}$$
$$\left\{ (1-2\delta)^2 (2\gamma - 1) \left[\frac{1}{4} - \frac{2}{3}(1-2\delta) + \frac{1}{2}(1-2\delta)^2 \right] + \frac{1}{12} - \frac{\gamma}{48} \right\} \tag{31}$$

For this time period the response is elastic.

For the time interval $1.5 < t < 2.0$ or $-2\kappa_{el} < \kappa < 0$, the response is again nonlinear, and the stress reads:

$$\sigma(y,t) = E\varepsilon_{el} \left\{ 2\frac{\kappa(t)}{\kappa_{el}}\frac{y}{h} - H\left(y - \frac{h}{4}\right) 2\left(2\frac{y}{h} - \frac{1}{2}\right)^2 + \right.$$
$$\left. H(y - y_*) \left[\frac{\kappa(t)}{\kappa_{el}}\frac{y}{h} - 2\left(\frac{y}{h} - 1\right) \right]^2 \right\} \tag{32}$$

where

$$y_* = \frac{h}{2}\frac{2\kappa_{el}}{2\kappa_{el} - \kappa(t)} \tag{33}$$

For this step again we have two regions. In the first region ($y_* > h(1-2\delta)/2$) plasticity takes place in the flange. Integrating stresses given by (32) yields to:

$$M(t) = E\bar{I}\kappa - 3EI\kappa_{el} \left\{ (2\gamma - 1)(1-2\delta)^2 \right.$$
$$\left. \left[\frac{1}{4} - \frac{2}{3}(1-2\delta) + \frac{1}{2}(1-2\delta)^2 + \frac{1}{12} - \frac{\gamma}{48} \right] \right\}$$

$$+EI\kappa_{el}\left[3\left(\frac{\kappa\left(t\right)}{\kappa_{el}}-2\right)^{2}\left(\frac{1}{16}-\frac{\kappa_{el}^{4}}{\left(2\kappa_{el}-\kappa\right)^{4}}\right)+\right.$$

$$\left.8\left(\frac{\kappa}{\kappa_{el}}-2\right)\left(\frac{1}{8}-\frac{\kappa_{el}^{3}}{\left(2\kappa_{el}-\kappa\right)^{3}}\right)+6\left(\frac{1}{4}-\frac{\kappa_{el}^{2}}{\left(2\kappa_{el}-\kappa\right)^{2}}\right)\right] \tag{34}$$

In the second region ($y_* < h(1-2\delta)/2$) elastic-plastic boundary falls in the web. Substituting (32) into (18) and taking integration similar to (4) it is obtained:

$$M\left(t\right)=E\bar{I}\kappa-3EI\kappa_{el}\left\{\left(2\gamma-1\right)\left(1-2\delta\right)^{2}\right.$$

$$\left\{\frac{\left(1-2\delta\right)^{2}}{2}\left[1-\frac{1}{8}\left(\frac{\kappa}{\kappa_{el}}-2\right)^{2}\right]-\frac{\left(1-2\delta\right)}{3}\frac{\kappa}{\kappa_{el}}-\frac{1}{4}\right\}+$$

$$\left.+\frac{1}{4}-\frac{\gamma}{48}+\frac{2}{3}\frac{\gamma\kappa_{el}^{2}}{\left(2\kappa_{el}-\kappa\right)^{2}}-\frac{1}{16}\left(\frac{\kappa}{\kappa_{el}}-2\right)^{2}-\frac{1}{3}\frac{\kappa}{\kappa_{el}}\right\} \tag{35}$$

The procedure for other steps is straight forward. The moment-curvature hysteretic loop is plotted in Fig.11. From all above expressions for moment-curvature relation for $\gamma = 1/2$, and $\delta = 1/2$ the results for rectangular cross section is recovered. This diagram is plotted in the same Fig.11. It is clear that rectangular cross section is much stiffer than rectangular tube.

5 Numerical analysis

In this Paragraph, the same problem of cyclic bending of rectangular box section, is analysed using Finite Element Method (FEM) and software package ABAQUS. Elastic-plastic analysis, including hardening of the material, is conducted. Hardening is assumed to be either isotropic or kinematic. In the case of isotropic hardening, the yield surface in the stress space expands, while neglecting the distortion and movement of its center. Yield surface for the case of kinematic hardening moves with work hardening, preserving its size and shape. The results presented here are obtained using isotropic hardening model.

FE model of the beam and its cross section are presented in Fig.13. Hexahedral elements with 20 nodes and reduced integration are used. Variable curvature is prescribed at both ends of the simply supported beam, and variation of the curvature during the time is the same as in Fig.9. The stresses for $\kappa = 2\kappa_{el}$ and residual stresses for $\kappa = 0$, obtained by numerical procedure, are shown in Fig.13. It can be seen that the results are very similar to those shown in Fig.10, even though ABAQUS uses different procedures to describe the plastic behaviour in comparison to the Preisach model presented here.

6 Conclusions

In the present paper it is shown, on new examples, that Preisach model has several advantages when it is applied to the problem of cyclic plasticity of axially loaded members and cyclic bending of beams as well. Mathematical rigor and a closed form analytical solutions makes the Preisach model very competitive with the other methods of solution. It is also shown that from results obtained for cyclic bending of rectangular tube section, the results for full cross section, which are obtained in the paper [3], can be recovered. As is shown previously, from results obtained in this paper Bauschinger s effect and Masing s law of cyclic plasticity are satisfied, both in case of axial loading and cyclic bending as well. Also results obtained by FEM using well know code ABAQUS are in agreement wit analytically obtained.

Acknowledgments: The authors gratefully acknowledge the financial support provided by Serbian Ministry of Science to UB, Department of Civil Engineering, through grants with numbers: OI 144027, 144037, 144038, which made this work possible.

D.S. is indebted to Prof. Dr. Dusan Krajcinovic not only for introducing him to Preisach model and Mayergoyz 1991, monograph, but for the permanent support throughout the years.

References

[1] Asaro, R.J., 1975, Elastic-plastic memory and kinematic type hardening, Acta Metall., 23, 1255-1265.

[2] Preisach, F.,1936, Uber die magnetishe Nachwirkung, Z. Phys., 94, 277-302.

[3] Sumarac, D., Stosic, S., 1996, The Preisach model for the cyclic bending of elasto-plastic beams, Eur. J. Mech., A/Solids, 15 (1), 155-172.

[4] Iwan, W.D., 1967, On a class of models for the yielding behaviour of continuous and composite systems, J. Appl. Mech., 34, 612-617.

[5] Lubarda, A.V., Sumarac, D., Krajcinovic, D., 1992, Hysteretic response of ductile materials subjected to cyclic loads. In: Ju, J.W. (Ed.) Recent Advances in damage Mechanics and Plasticity, ASME Publication, AMD, 123, 145-157.

[6] Lubarda, A.V., Sumarac, D., Krajcinovic, D., 1993, Preisach model and hysteretic behaviour of ductile materials. Eur. J. Mech., A/Solids, 12, n^0 4, 445-470. 145-157.

[7] Mayergoyz, I. D., 1991, Mathematical Models of Hysteresis, Springer-Verlag, N.Y., 1-140.

[8] ABAQUS Analysis User's Manual, 2006, ABAQUS Inc., USA

Submitted on February 2008.

Modeliranje histerezisnog ponašanja elastoplastičnih materijala

U posmatranom radu Prajzakov model histerezisa je primenjen na modeliranje cikličnog ponašanja elasto-plastičnih materijala. Pri tome brzina nanošenja opterećenja i viskozni efekti se ne uzimaju u obzir. U radu se detaljno proučava problem aksijalnog naprezanja pravougaonog poprečnog preseka i ciklično savijanje pravougaone čelične cevi. Konstruisana je histerezisna petlja za zadatu promenu cikličnog opterećenja za materijal modeliran sa tri osnovna elementa. Takodje, histerezis momenat-krivina za čeličnu pravougaonu cev je konstruisan za zadatu istoriju promene krivine. U posebnom poglavlju se obradjuju rezultati dobijeni primenom MKE korišćenjem programa ABAQUS. Svi dobijeni rezultati jasno pokazuju prednost Prajzakovog modela kod opisivanja cikličnog ponašanja elasto-plastičnih materijala.

doi:10.2298/TAM0803287S Math.Subj.Class.: 34C55, 74C05, 74S05